Tribol Lett (2008) 32:159–170
DOI 10.1007/s11249-008-9374-6

ORIGINAL PAPER

Microstructural and Tribological Properties of A356 Al–Si Alloy Reinforced with Al_2O_3 Particles

Aleksandar Vencl · Ivija Bobić · Milan T. Jovanović · Miroslav Babić · Slobodan Mitrović

Received: 20 August 2008 / Accepted: 26 September 2008 / Published online: 1 November 2008

Abstract In the present study, the effect of the Al_2O_3 particles (average size of 12 μm, 3 and 10 wt.%) reinforcement on the microstructure and tribological properties of Al–Si alloy (A356) was investigated. Composites were produced by applying compocasting process. Tribological properties of unreinforced alloy and composites were studied, using pin-on-disc tribometer, under dry sliding conditions at different specific loads and sliding speed of 1 m/s. Microhardness measurements, optical microscope and scanning electron microscope were used for microstructural characterization and investigation of worn surfaces and wear debris. During compocasting of A356 alloy, a transformation from a typical dendritic primary phase to a non-dendritic rosette-like structure occurred. Composites exhibited better wear resistance compared with unreinforced alloy. Presence of 3 wt.% Al_2O_3 particles in the composite material affected the wear resistance only at specific loads up to 1 MPa. The wear rate of composite with 10 wt.% Al_2O_3 particles was nearly two order of the magnitude lower than the wear rate of the matrix alloy. Dominant wear mechanism for all materials was adhesion with others mechanisms: oxidation, abrasion and delamination as minor ones.

Keywords Compocasting · Al–Si alloy · Al_2O_3 particles · Dry sliding · Friction · Wear

1 Introduction

The use of different types of metal matrix composites (MMCs) is constantly growing because they possess better physical, mechanical and tribological properties compared to the matrix materials. Composite materials based on light metals like aluminium, magnesium and zinc find application in many industries due to their low density [1–5].

The idea that a relatively small amount of reinforcement can improve characteristics of matrix material is attractive, and constant improvements of MMCs technological processing and possibilities for their new applications are not a surprise. Numerous authors investigated friction and wear properties of aluminium matrix composites studying the influence of different parameters, such as:

- the type of the matrix and counter body material and their hardness [6–8],
- the type of the reinforcements, their shape, size and volume fraction [9–11] and
- testing conditions (load, speed, temperature, type of relative motion, lubrication and environment) [12–14].

Most of these investigations were conducted on model type pin-on-disc tribometers. A more detailed review of the apparatus, materials and testing conditions used can be found elsewhere [15, 16].

The results obtained from the applied load and reinforcement content effects on friction and wear properties of

A. Vencl (✉)
Tribology Laboratory, Mechanical Engineering Faculty, University of Belgrade, Kraljice Marije 16, 11120 Belgrade 35, Serbia
e-mail: avencl@mas.bg.ac.yu

I. Bobić · M. T. Jovanović
Department of Materials Science, Institute of Nuclear Sciences "Vinča", P.O. Box 522, 11001 Belgrade, Serbia

M. Babić · S. Mitrović
Tribology Laboratory, Mechanical Engineering Faculty, University of Kragujevac, Sestre Janjić 6, 34000 Kragujevac, Serbia

various aluminium alloys and their composites, under dry sliding conditions, indicate existence of critical transition behaviour from mild to severe wear [10–12, 17, 18]. Improvements of the wear resistance of aluminium MMCs were more than one order of the magnitude compared with matrix materials at low contact pressures.

The addition of reinforcements improves the critical transition values of applied load and wear resistance compared with corresponding matrix alloy, and this improvement is achieved with the addition of up to ~20 vol.% of reinforcement [10, 16, 17]. However, increase of the volume fraction can also provoke clustering of the particles during fabrication of the composite [17]. Strength of particles/matrix interface is very important parameter since that interfaces could be relatively weak due to interfacial reaction and poor wettability. If the reinforcement is well bonded to the matrix, the composite wear resistance increases continuously with increasing volume fraction of reinforcement. In contrast, if the reinforcement is not well bonded to the matrix, the wear resistance of the composite increases up to a critical amount of the reinforcement and thereafter starts to decrease [18].

The A356 alloy belongs to a group of hypoeutectic Al–Si alloys with a wide range of applications in the automotive and avionic industries. This alloy is used in the heat-treated condition in which an optimal ratio of physical and mechanical properties is obtained [19]. The alloy solidifies in a broad temperature interval (48 °C) [20] and is suitable for the treatment in the semi-solid state as well as as-cast condition [21]. Due to these properties, investigations were directed to the rheological behaviour [22] and assessment of optimal parameters for semi-solid processing of this alloy [21, 23]. Applying these processing, it was possible to obtain castings with reduced porosity, non-dendritic structure and good mechanical properties.

The object of this paper was to study the effect of the Al_2O_3 particles reinforcement on the microstructure and tribological properties in dry sliding conditions of the non-modified A356 matrix alloy.

2 Experimental Procedure

2.1 Preparation of the Composites

The matrix material was A356 hypoeutectic Al–Si alloy (EN AlSi7Mg0.3) with the chemical composition shown in Table 1. Alloy was cast into a cold graphite mould, and ingot with 12 mm in diameter and 100 mm in height was produced. No grain refinement treatment was performed during the process of casting.

Composites were produced by the compocasting process using mechanical mixing of the matrix, i.e. Al_2O_3 particles

Table 1 Chemical composition (wt.%) of A356 Al–Si alloy

Element	Si	Cu	Mg	Mn	Fe	Zn	Ni	Ti	Al
Percentage	7.20	0.02	0.29	0.01	0.18	0.01	0.02	0.11	Balance

as reinforcement were added into the semi-solid A356 alloy by infiltration and admixing. The average size of Al_2O_3 particles was 12 μm, whereas the amount of particles was 3 and 10 wt.%. The apparatus for the compocasting processing (Fig. 1) consists of a laboratory electric 2 kW resistance furnace (with additional temperature control equipment) and a mixer with a plate-like active part, fixed on the mixer shaft. Thermocouple was inserted 20 mm above the bottom of the alumina crucible through the small opening in the crucible wall. With installed electronic equipment, it was possible to record and to change the mixing rate. Processing temperature was ~600 °C. The time of infiltration and mixing as well as mixing rates were adjusted according to the amount of the reinforcement.

The semi-solid melt of the composite was poured into a prepared steel mould heated at 500 °C. Subsequent pressing was applied in order to obtain casting (36 mm in diameter and 150 mm in height) with maximum density. Samples for metallographic investigation were machined from these castings. In order to obtain specimens for microhardness measurements and tribological tests, the semi-solid melt was additionally pressed with normal load of 60 kN, at the temperature of 570 °C in a special mould made of IN 100 superalloy. Specimens for these tests were cut from the "head" of the tensile test sample (schematically illustrated in Fig. 2). Results of tensile tests are not reported in this paper.

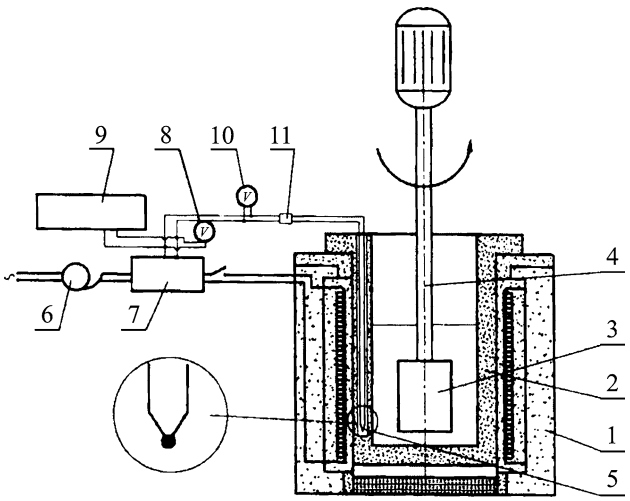

Fig. 1 Schematic drawing of the apparatus for compocasting processing (1—resistance furnace, 2—crucible, 3—mixer, 4—mixer shaft, 5—thermocouple and from 6 to 11—devices and instruments for temperature measurement, control and regulation)

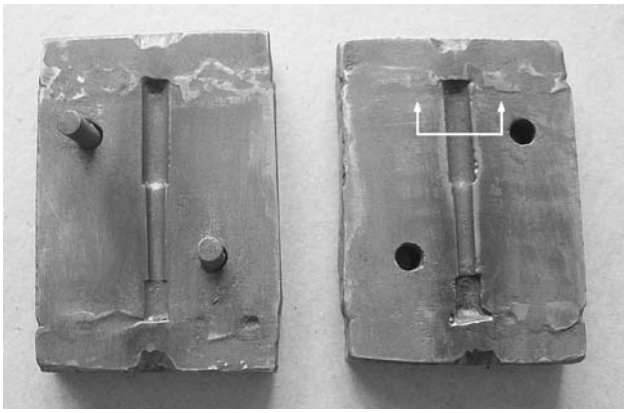

Fig. 2 Mould for test samples (arrows denote part of the sample cut for microhardness measurements and tribological tests)

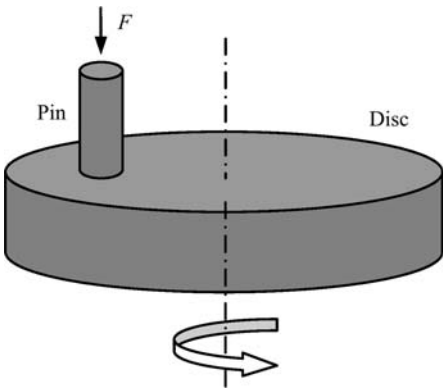

Fig. 3 Schematic drawing of the pin-on-disc tribometer

Three sets of specimens were used for testing: one was fabricated from the matrix material (referred as A356) and the other two from the composite material with 3 and 10 wt.% Al_2O_3 (referred as 3–12 and 10–12, respectively). All specimens were subjected to heat treatment with following parameters: solution annealing at 540 °C for 6 h, water quenching and arti cial ageing at 160 °C for 6 h.

2.2 Methods of Characterization

Microstructural and mechanical characterization of both matrix material and composites included metallographic examinations with optical microscope (OM) and hardness measurements. Metallographic samples were prepared in a standard way applying grinding and polishing, whereas etching in Keller's solution (the mixture of 95 ml H_2O, 2.5 ml HNO_3, 1.5 ml HCl and 1 ml HF) was used to reveal the microstructure. Microhardness measurements were carried out using a 1,368 Vickers diamond pyramid indenter and 50 g load. At least six measurements were made for each specimen in order to eliminate possible segregation effects and to get a representative value of the material microhardness. Density of the specimens was measured by Archimedes method.

Tribological tests were carried out on the pin-on-disc tribometer under dry sliding conditions at room temperature. Cylindrical pins of tested materials with 2.5 mm in diameter and 30 mm in length were used as wear test specimens. Disc (hereafter referred to as a counter body) of 100 mm in diameter and 10 mm thick was made of nodular grey cast iron. This material was chosen as a standard piston ring material with speci cation according to the ISO standard (Subclass Code MC 5210) and hardness of 220 HV_{10}. Schematic drawing of load, pin, counter body and direction of the rotation is shown in Fig. 3. Surface roughness of pins and the counter body was approximately $R_a = 0.5$ and 0.3 μm, respectively.

Before and after testing, both the pin and the counter body were degreased and cleaned with benzene. To calculate the mass loss, pins were weighed by electronic balance with an accuracy of 10^{-4} g, before and after each test. The value of friction force was monitored during the test and through the data acquisition system stored in the PC, enabling the calculation of the friction coef cient. The parameters of the tribological tests were as follows: sliding speed of 1 m/s, sliding distance of 5,000 m and normal load from 2.5 to 20 N. Taking into account the contact area of ~ 5 mm^2, the applied pressure, designated as a speci c load, was in the interval between 0.5 and 4 MPa.

Wear tracks on the counter body, worn surface of pins and generated wear debris after testing were examined with OM and scanning electron microscope (SEM) equipped with energy dispersive spectrometer (EDS).

3 Results

3.1 Microstructure, Microhardness and Density

The results of metallographic investigation of the matrix alloy and composites are illustrated in Fig. 4. The microstructure of the matrix alloy consists of fully dendritic primary α phase and a eutectic in interdentritic area (Fig. 4a). Compocasting process produced morphological changes in the microstructure, i.e. the microstructure of composites is distinguished by large primary α phase rosettes (Fig. 4b, c). Signi cant coarsening of the α phase occurred during compocasting. Al_2O_3 particles reinforcement are visible not only in the eutectic zone but are in ltrated in the α phase primary particles as well.

The results of microhardness and density measurements are shown in Table 2. Microhardness and density increase with addition of Al_2O_3 particles. Microhardness also increases after heat treatment and 10–12 composite exhibits the highest values.

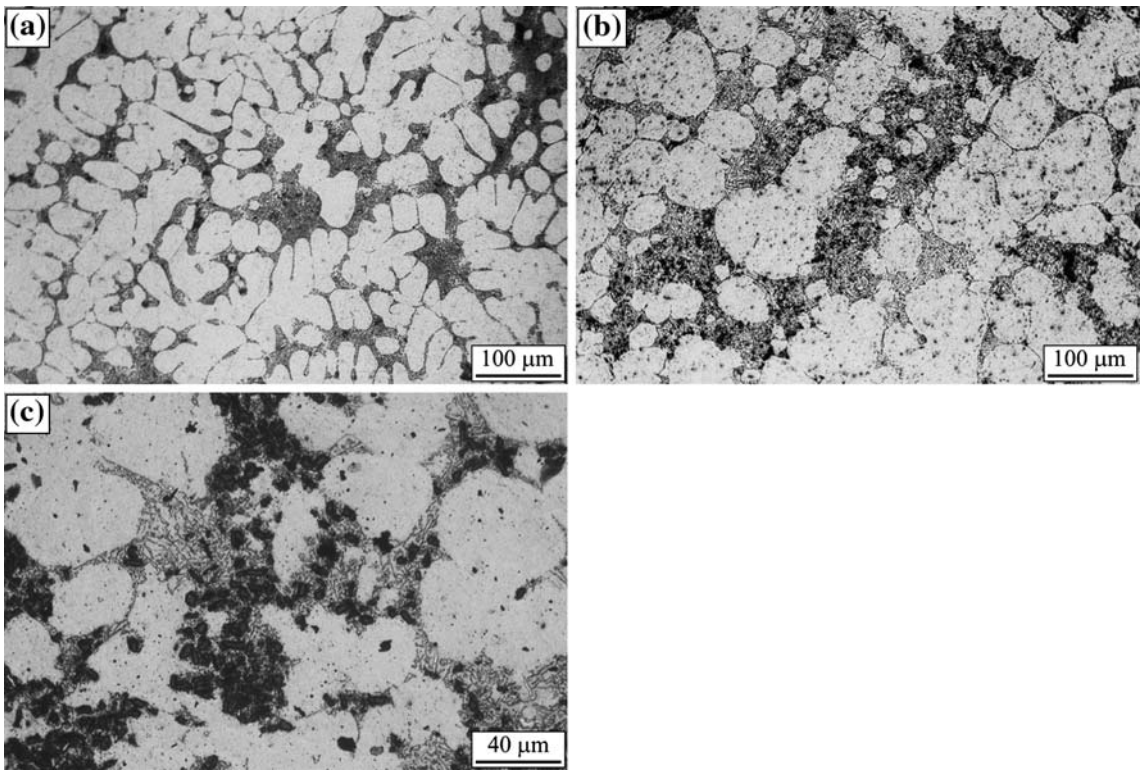

Fig. 4 Microstructures of the heat treated and etched specimens: a A356 matrix alloy, b 3–12 and c 10–12 composites

Table 2 Microhardness and density of matrix alloy and composites[a]

Properties	A356		Composites			
			3–12		10–12	
Microhardness ($HV_{0.05}$)	As-cast	Heat treated	Compocast	Heat treated	Compocast	Heat treated
	62	70	73	80	85	95
Density (g/cm^3)	2.67		2.70		2.78	

[a] Average result of six measurements

3.2 Tribological Tests

The wear tests results show that the mass loss as a function of the sliding distance increases with the increase of specific load (Fig. 5). Generally, it could be noticed that some wear curves show two distinct slopes, which correspond to the initial (run-in) period and the steady-state period. Matrix alloy shows linear dependence of the mass loss from the sliding distance for the whole applied load interval (Fig. 5a). The same dependence of the mass loss from the sliding distance also shows 3–12 composite, but only at higher specific loads (Fig. 5b). This linear dependence of the mass loss from the sliding distance corresponds to the steady-state period. Wear curves of the 3–12 composite, at lower specific loads, and wear curves of 10–12 composite, for the whole applied load interval, show somewhat different shape, i.e. before the onset of the usually lower and linear steady-state wear, run-in wear appears as the initial high-rate transient wear (Fig. 5c). The transition from run-in to steady-state period is denoted with arrows on the wear curves. Duration of run-in period is relatively short and it decreases with the increase of specific load.

The wear rates (calculated for the steady-state period) of tested materials at different specific loads are presented in Fig. 6. The wear rate increases with the increase of specific load and decreases with the increase of Al_2O_3 particles amount. The wear rate of 10–12 composite is nearly two order of the magnitude lower than the wear rate of matrix alloy. Presence of 3 wt.% Al_2O_3 particles in the composite material affects the wear rate only at specific loads up to 1 MPa, and with higher loads, the wear rate abruptly increases becoming similar to the matrix alloy indicating the transition of the wear regime.

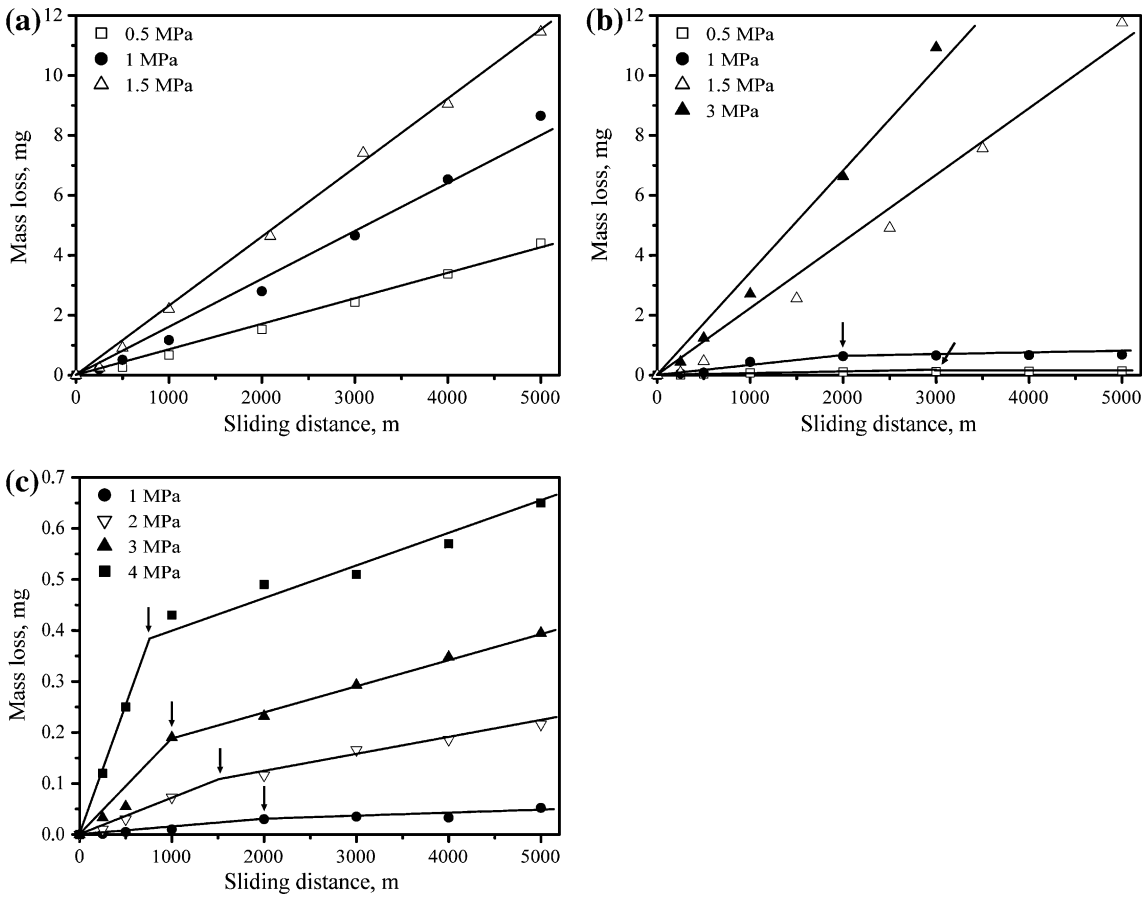

Fig. 5 Wear curves of a A356 matrix alloy, b 3–12 and c 10–12 composites at different speci c loads

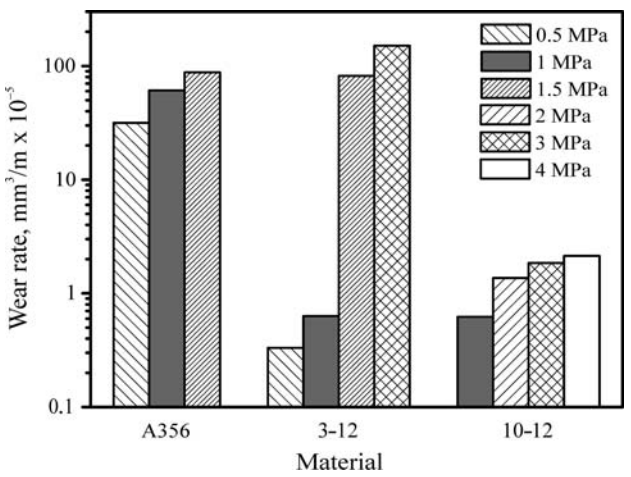

Fig. 6 Steady-state wear rates of tested materials at different speci c loads

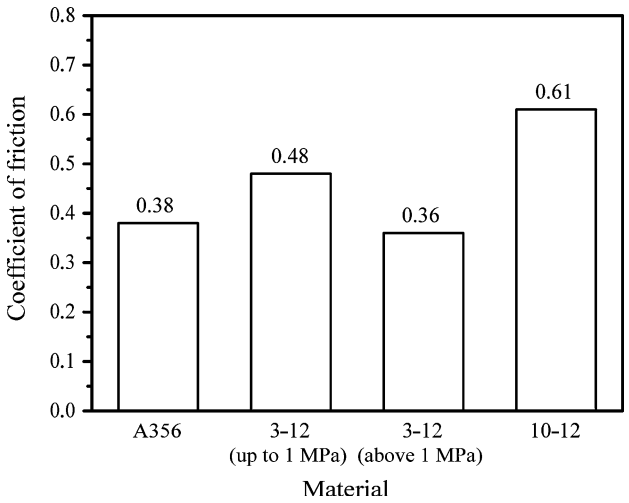

Fig. 7 The coef cient of friction average values of tested materials

Figure 7 illustrates average values of the steady-state friction coef cient of tested materials. Coef cient of friction of matrix alloy and 10–12 composite did not change signi cantly with the change of speci c load, and one mean value could be accepted for the whole applied load interval. On the other side, the friction coef cient of 3–12 composite decreased signi cantly at speci c loads above 1 MPa and reached the value very similar to the value of matrix alloy. Generally the value of the coef cient of friction increases with the amount of Al_2O_3 particles in the material.

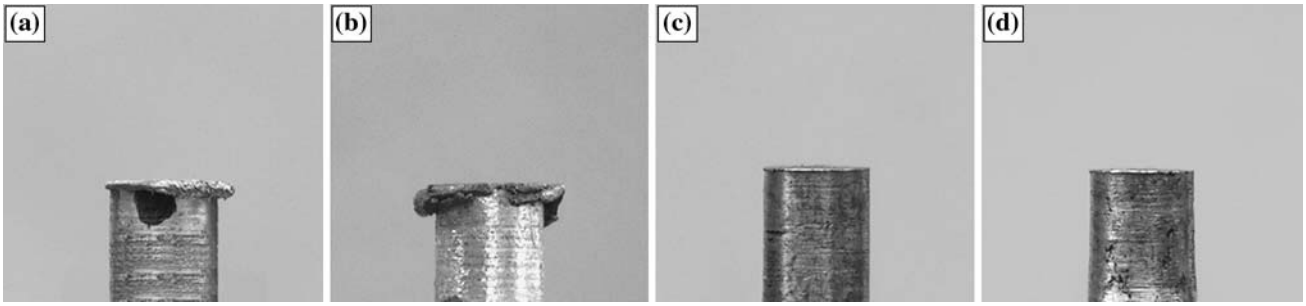

Fig. 8 The appearance of the pin contact surface of tested materials as a function of applied specific load: **a** A356 matrix alloy at 1 MPa, **b** 3–12 composite at 1.5 MPa, **c** 3–12 composite at 1 MPa and **d** 10–12 composite at 4 MPa

3.2.1 *Worn Surfaces and Wear Debris*

Condition of pin contact surfaces was observed during the tests as well as at the end of tests and recorded with camera (Fig. 8). Plastic flow of material on the surface of some pins was noticed. This plastic flow at A356 matrix alloy was present, more or less intensive depending on the specific load, for the whole applied load interval (Fig. 8a). Material plastic flow usually occurred in the early stage of the test (after 250 or 500 m) and continued to grow with sliding distance. For 3–12 composite, plastic flow of material on pin surface was present only at higher specific loads (above 1 MPa) (Fig. 8b), while it was neither noticed at lower specific loads (up to 1 MPa) (Fig. 8c) nor at 10–12 composite for the whole applied load interval (Fig. 8d). It has also been noticed that the worn surfaces were covered with the brown layer.

SEM micrographs of pins worn surfaces at the end of tests are presented in Fig. 9. Worn surfaces of matrix alloy (Fig. 9a, b) and 3–12 composite at higher specific loads (Fig. 9c, d) showed similar appearance. Presence of distinct grooves originates from the ploughing of the pin surface. These grooves are wider in the 3–12 composite (Fig. 9c) than in the matrix alloy (Fig. 9a). Fine scoring marks (denoted by arrows in Fig. 9c) may be due to the abrasion of Al_2O_3 particles entrapped in wear debris. Presence of wear debris caused by fracture, accumulated into the adhesive wear pits was also noticed (Fig. 9d). Smearing as a result of material plastic flow appears in the matrix alloy as well as in the 3–12 composite at higher specific load (Fig. 9b, d). This smearing and material plastic flow was also noticed on the macro level (Fig. 8a, b). Propagation of small cracks in radial direction is visible in plastically deformed regions (denoted by arrows in Fig. 9b, d). On the other side, worn surfaces of 3–12 composite at lower specific loads were similar to the worn surfaces of 10–12 composite (Fig. 9e, f). There was no presence of grooves, while presence of the transferred material from the counter body is visible (Fig. 9e). Formation of deep caverns could also be noticed (denoted by arrows in Fig. 9f).

The appearance of the counter body worn surfaces is presented in Fig. 10. Presence of the transferred pin material from A356 matrix alloy and 3–12 composite (at higher specific loads) to the counter body surface could be noticed (Fig. 10a, b). As for 3–12 composite (at lower specific loads) and 10–12 composite, there was no significant transfer of pin material to the counter body and only wide grooves on the counter body surface could be noticed (Fig. 10c, d). In the opposite direction, however, transfer of material from the counter body was observed on the worn surface of these specimens (see black spots in Fig. 11a). According to Fig. 11b and corresponding EDS results (Fig. 11c–g), it is evident that these black spots represent iron transferred from the counter body to the pin surface. Minor extent of oxygen was also detected on the worn surfaces.

Morphology and size of wear debris collected during the tests are shown in Fig. 12. Debris generated by the wear of the materials in contact (counter body and corresponding specimen) originate mostly from the pin material. Among the wear debris of A356 matrix alloy and 3–12 composite, at higher specific loads prevail mainly sharp edge, plate-like particles (Fig. 12a, b). On the surface of these plate-like particles, presence of material plastic flow could be noticed. Size of the particles was from 20 to 30 μm. In some cases, individual long, rod-like particles, longer than 50 μm, may be seen. In the case of 3–12 composite (at lower specific loads) and 10–12 composite, wear debris are also mainly sharp edge, plate-like particles, without any visible grooves on them (Fig. 12c). Size of these particles was rather smaller than the others with ~10 μm in diameter. In some cases, particles from 20 to 30 μm in diameter, may be seen. Some particles in wear debris of 3–12 composite (at lower specific loads) and 10–12 composite were brown coloured indicating formation of the iron oxides and existence of the oxidation wear.

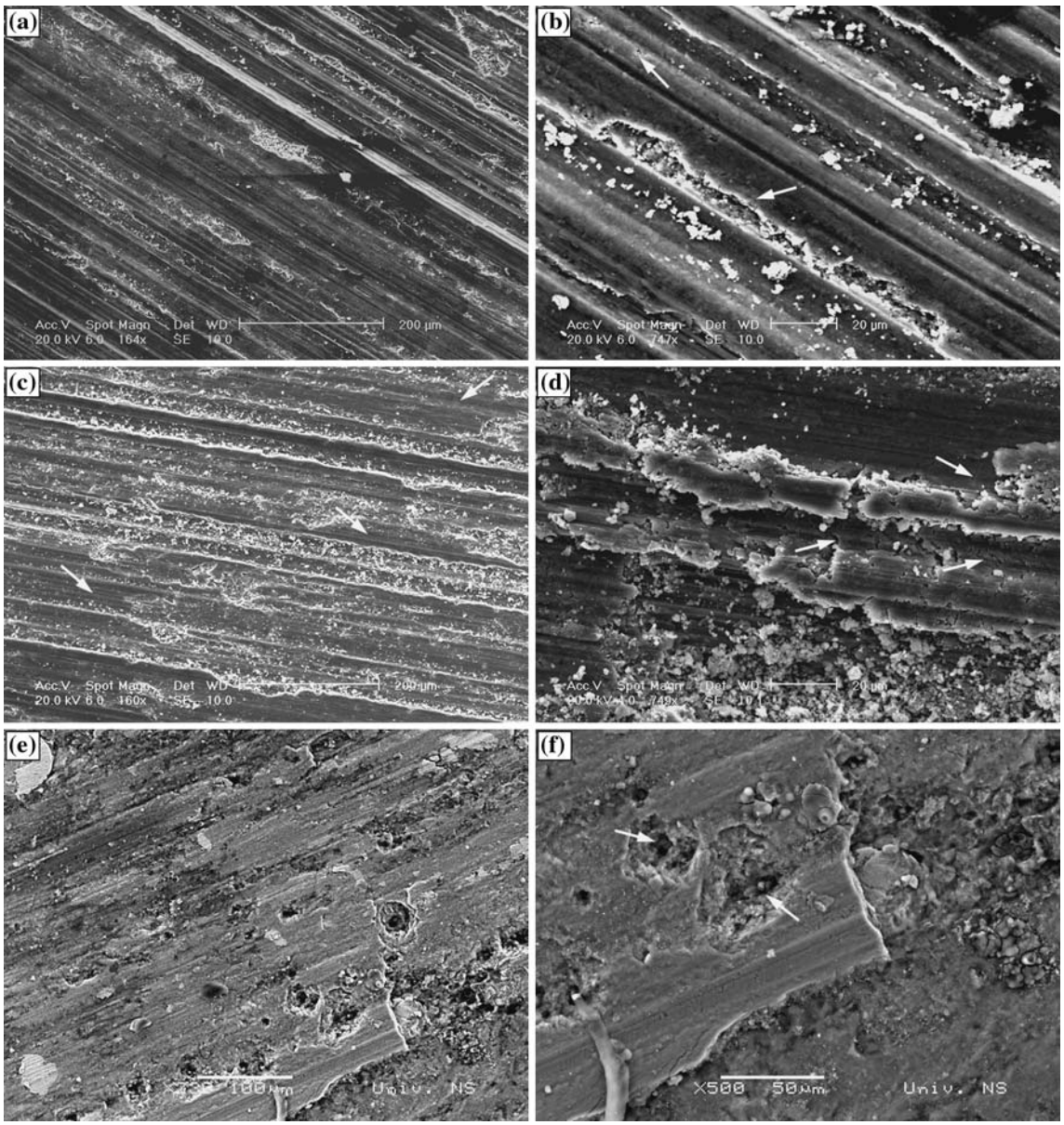

Fig. 9 SEM micrographs of the pins worn surfaces (a) and (b) A356 matrix alloy at 1.5 MPa, (c) and (d) 3–12 composite at 1.5 MPa and (e) and (f) 10–12 composite at 1 MPa

4 Discussion

At the end of solidification, the microstructure of the matrix alloy consists of primary aluminium-rich dendrites of the α phase and the interdendritic eutectic in the region between the α phase (Fig. 4a). Microstructure of composites (Fig. 4b, c) suggests that during the compocasting process a transformation from a typical dendritic to a non-dendritic structure of the primary α phase occurred as a result of shear forces generated by the mixer rotation. Infiltration of reinforcement particles into the primary α phase, which appear below the liquidus temperature and during mixing is obviously result of collisions and interactions of the α phase and Al_2O_3 particles. The remainder of the reinforcement was pushed to the eutectic zone consisting of α phase, rod-like silicon particles and Al_2O_3 particles mixture (Fig. 4d). The size and the shape of the separated silicon particles in eutectic determine the morphology of eutectic, which has a great effect on the mechanical properties of the alloy. Apart from the reinforcing effect of Al_2O_3 particles, the increase of hardness with ageing is the result of the precipitation of β' particles (Mg_2Si) or S-phase (Al_2CuMg) [25].

From Table 2, it can be seen that the hardness of tested materials increases with increase of Al_2O_3 particles amount. Straffelini et al. [26] found that the matrix

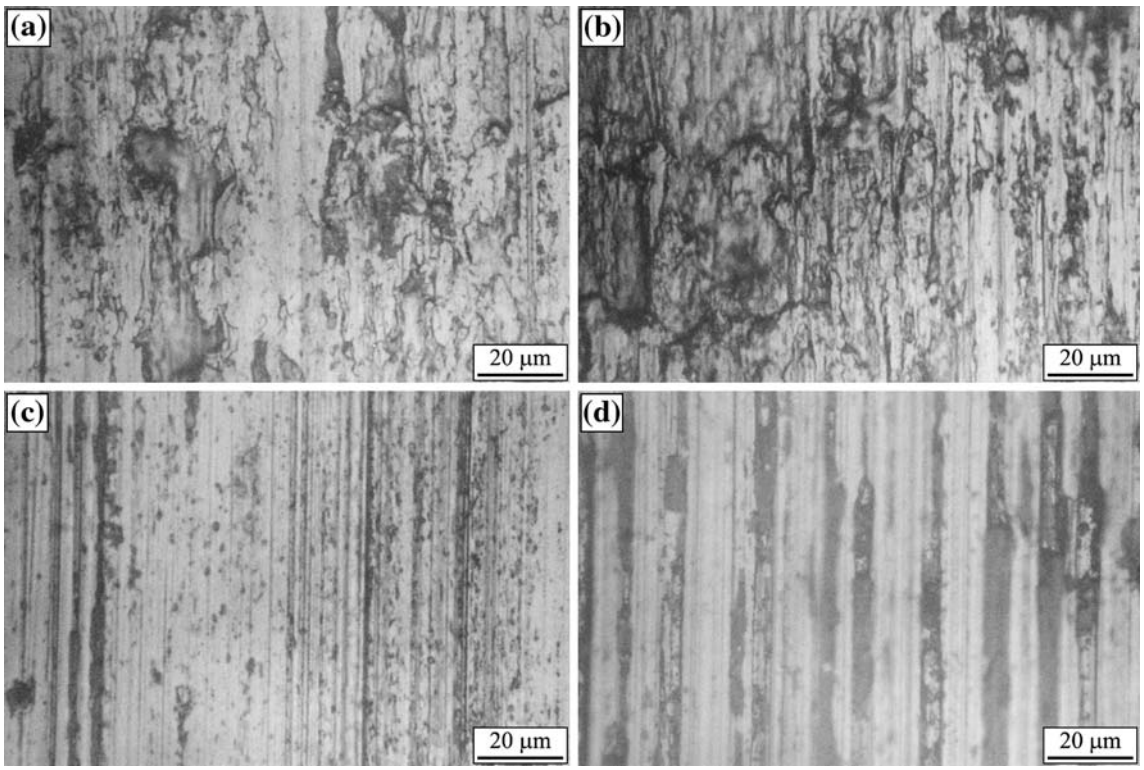

Fig. 10 OM micrographs of the counter body worn surfaces: a counter body versus A356 matrix alloy at 1 MPa, b counter body versus 3–12 composite at 3 MPa, c counter body versus 3–12 composite at 1 MPa and d counter body versus 10–12 composite at 3 MPa

hardness exerts a strong in uence on the dry sliding wear behaviour of Al_2O_3 particles reinforced composite, and that the composite with the lowest matrix hardness displays the lowest wear rate. On the other side, García Cordovilla et al. [7] con rms that the higher hardness of the composite materials was associated to a lower wear rate, but the dependence was not linear. In the present investigation, the wear rate is also considered to be inversely proportional to the hardness of the material and this is con rmed by the results of the total wear rate on hardness dependence (Fig. 13).

The applied load has a signi cant in uence on the wear rate of tested materials (Fig. 6). In general, with increase of the applied speci c load the wear rate of the matrix alloy and composites also increases. Matrix alloy (for the whole applied load interval) and 3–12 composite (at speci c loads higher than 1 MPa) show very intensive wear rate from the beginning of the test, with very short or without any run-in period. Wear behaviour was determined by extensive material plastic ow on pin surface (Fig. 8a, b) indicating severe wear regime as dominant. These plastic deformations are unwelcome and represent the limiting factor for tribological application of these materials. However, 3–12 composite (at speci c loads up to 1 MPa) and 10–12 composite (for the whole applied load interval) did not show plastic deformation of the pin surface (Fig. 8c, d) exhibiting the lower values of the wear rates. This suggests that in 3–12 composite a critical load of 1 MPa exists above, which Al_2O_3 particles are not able to sustain the applied load, i.e. particles near the contact surface act no longer as load carrying elements and the wear rate is mainly controlled by the matrix alloy. The critical load indicates the transition from mild to severe wear regime characterized with deformation and material plastic ow on pin surface.

Enhanced amount of Al_2O_3 particles prevents severe wear by protecting the soft matrix and improving wear resistance. Thus, if the particles remain well bonded with the matrix during sliding, the aluminium matrix that surrounds the particulates will be worn away, and essentially all contact will be between the reinforcing particles and the counter body. All forces developed during sliding will be preserved in contact between Al_2O_3 particles and the counter body, and for this reason, the shear stress at the Al_2O_3 particle/matrix interface may cause particle decohesion. The wear rate will be then largely controlled by the wear rate at which particles decohere [10]. For the investigated composites, especially in the case of 10–12 composite, the most important in uence on the wear rate demonstrates the presence of Al_2O_3 particles with the hardness much higher than the matrix alloy. The amount of 10 wt.% Al_2O_3 particles provides protection of the matrix

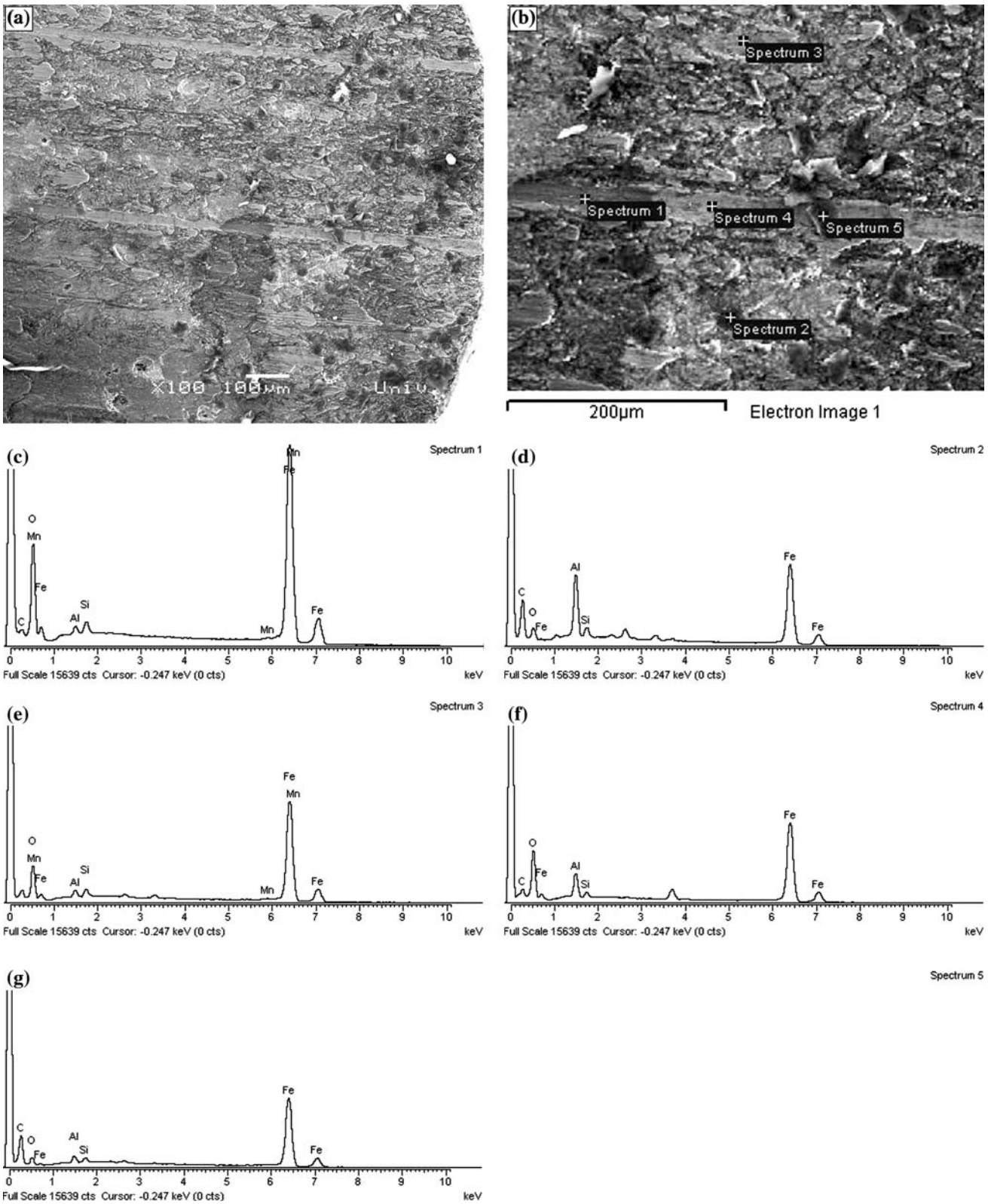

Fig. 11 SEM microphotograph and EDS analysis of 10–12 composite pin worn surface at 4 mm transferred material from the counter body to the pin surface and b–g EDS analysis of corresponding spots

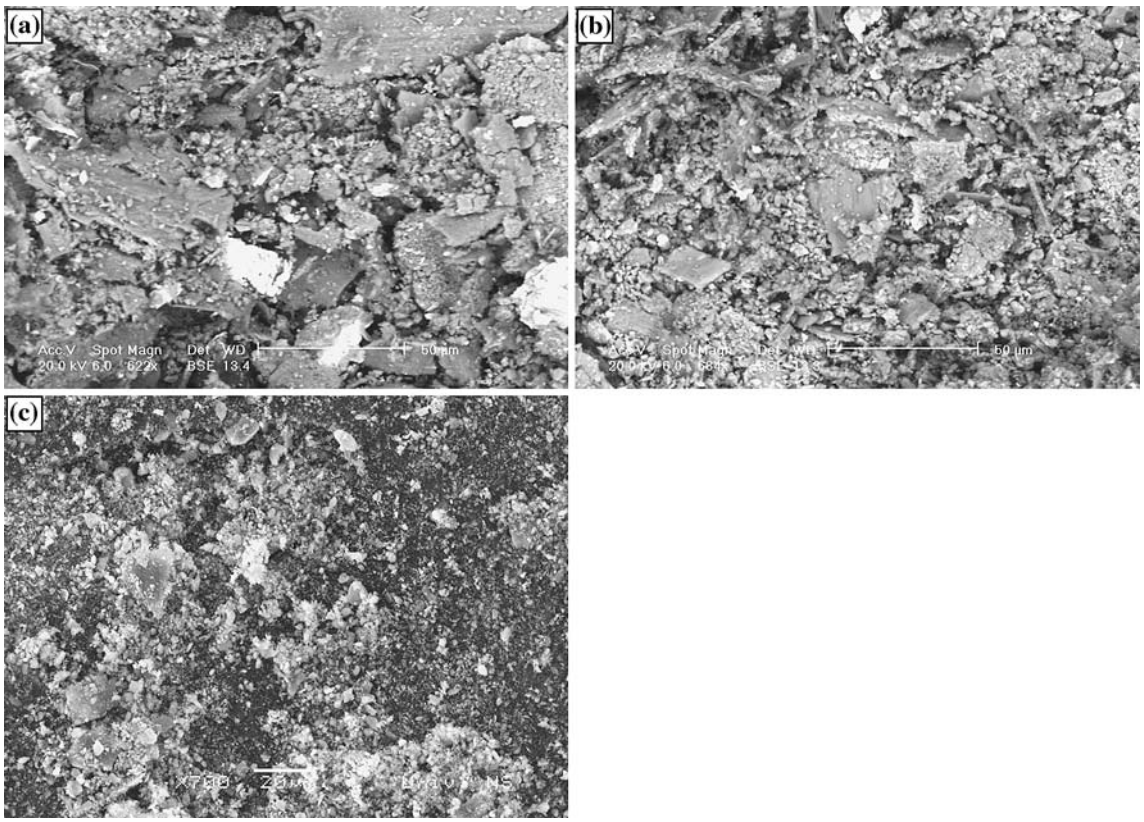

Fig. 12 SEM microphotographs of the wear debris generated in contact of counter body with: a A356 matrix alloy at 1.5 MPa, b 3–12 composite at 1.5 MPa and c 10–12 composite at 2 MPa

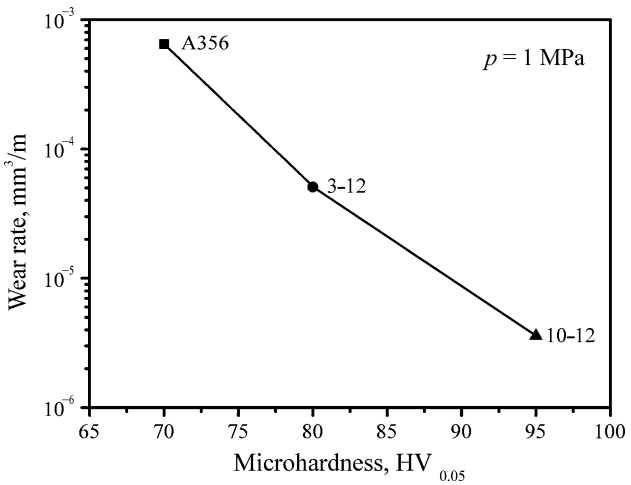

Fig. 13 The dependence of the total wear rate on microhardness

alloy during sliding, thus limiting the deformation and penetration of the counter body into the surface of the composite. In comparison with the matrix alloy, the wear rate of 10–12 composite is therefore much improved with addition of Al_2O_3 particles.

The unreinforced matrix alloy is much softer than the counter body material and during sliding counter body penetrates into the matrix alloy producing deep grooves and causing extensive plastic deformation of the surface (Fig. 9a, b), which results in great material loss and significant wear rate. The worn surfaces also contain the evidence of adhesive wear in the form of adhesive pits. On the other side, the large scale of the matrix alloy is transferred to the counter body (Fig. 10a). The worn surfaces of 3–12 composite, at higher specific load, were somewhat similar to that of matrix alloy (Fig. 9c, d), i.e. they are characterized by grooves, extensive plastic deformation and adhesive wear pits (with accumulated wear debris). Transfer of 3–12 composite material to the counter body was also noticed (Fig. 10b). SEM microphotographs of the matrix alloy (Fig. 12a) and 3–12 composite, at higher specific load (Fig. 12b), indicate that the particles in the wear debris are mainly plate-like, with sharp edges, which are typical for adhesive wear [27, 28]. Presence of the rod-like particles, longer than 50 μm indicates existence of severe wear [29]. Analyses of pin and counter body worn surfaces condition and generated wear debris show that the predominant mechanism of wear was adhesion followed with plastic deformation.

On the other side, worn surfaces of 3–12 composite at lower specific loads were similar to worn surfaces of 10–12

composite (Fig. 9e, f). There was no presence of grooves. Presence of transferred material from the counter body (Fig. 9e) is confirmed with the EDS analysis (Fig. 11). Sporadic deep caverns formed by the pull outs of Al_2O_3 particles from the matrix (Fig. 9f) indicate relatively weak interfacial bonding between aluminium matrix and Al_2O_3 particles in these areas. These Al_2O_3 particles, fractured into fragmented pieces, have been entrapped between the pin and counter body and together with protruded Al_2O_3 particles from the matrix act as abrasives. This was confirmed with the counter body wear tracks surface observation, where presence of wide grooves was noticed (Fig. 10c, d). Presence of brown layer on the pins worn surface as well as brown-coloured wear debris indicate formation of the iron oxides and existence of the oxidation wear. SEM microphotographs of 10–12 composite (Fig. 12c) indicate that particles in the wear debris are also mainly plate-like, with sharp edges, which are typical for adhesive wear. Generally, the wear debris is finer than those from the matrix alloy and 3–12 composite (at higher specific load). Presence of the particles with 20 to 30 μm in diameter, i.e. less than 50 μm in diameter indicates that severe wear did not occur [29]. Analyses of pin and counter body worn surfaces condition and generated wear debris show presence of the steady-state mild wear. Dominant wear mechanism was adhesion, with others mechanisms: oxidation, abrasion and delamination as minor ones.

Attained friction coefficient values of the matrix alloy and composite materials were in expected range for light metals in dry sliding conditions. Increase of the coefficient of friction with the amount of reinforcement particles (Fig. 7) is ascribed to the fact that the amount of protruded Al_2O_3 particles increases during wear occupying larger area of pin surface. In the same time, one part of protruded Al_2O_3 particles are torn away from the matrix and fractured into fragmented pieces. In this situation, the contact between hard Al_2O_3 particles and the counter body material was established, resulting in higher values of the coefficient of friction. Compared with the matrix alloy, higher coefficient of friction values of 3–12 composite (only at lower specific loads) and 10–12 composite (for the whole specific load interval) correspond to lower values of the wear rate (see Fig. 6). Relatively low friction coefficient values of the matrix alloy and 3–12 composite (at higher loads) are due to the fact that at applied specific load pin surfaces of these two materials start to deform plastically and to flow (Fig. 8a, b). This plastic flow of the material reduces the value of the coefficient of friction. Transition of wear regime could also be identified by the coefficient of friction, i.e. the coefficient of friction of 3–12 composite abruptly decreases at specific loads above 1 MPa indicating the transition from mild to severe wear.

5 Conclusions

The microstructure of the A356 matrix alloy consists of primary aluminium-rich dendrites of α phase and the interdendritic eutectic in the region between α phase. Microstructure of composites suggests that during the compocasting process the transformation from a typical primary dendritic α phase to a non-dendritic rosette-like structure occurred as a result of the shear forces generated by the mixer rotation.

Presence of the critical load of 1 MPa, at which transition from the mild to the severe wear occurs, was observed for the composite material with 3 wt.% Al_2O_3 reinforcement. Above the critical load, this amount of Al_2O_3 reinforcement is not anymore able to carry the applied load. Particles near the contact surface fracture and act no longer as load carrying elements, so the wear rate is mainly controlled by the matrix alloy.

Significant improvement of the wear resistance for the composite material with 10 wt.% Al_2O_3 over the matrix alloy was nearly two order of the magnitude. Improvement of the wear resistance for the composite material with 3 wt.% Al_2O_3 was significant only at specific load up to 1 MPa. Composite material with higher amount of Al_2O_3 reinforcement showed better wear resistance since it possesses higher load carrying capacity of the hard reinforcement particles, which limits the amount of plastic deformation of the matrix.

Values of the friction coefficient of the matrix alloy and composite materials were in expected range for light metals in dry sliding conditions. Increase of the friction coefficient with the amount of Al_2O_3 reinforcement was ascribed to the higher amount of protruded Al_2O_3 particles occupying larger area of pin surface during wear. The higher coefficient of friction was the consequence of established contact between hard Al_2O_3 particles and the counter body material.

Dominant wear mechanism for all materials was adhesion, with others mechanisms: oxidation, abrasion and delamination as minor ones. Plastic deformation occurred when the applied specific load was higher from the critical value.

Acknowledgment The results of this paper are realized through the national project TR–6303B financially supported by the Ministry of Science of the Republic of Serbia (coordinator of project Prof. Dr. Miroslav Babić). Help from the partner of the project (Petar Drapšin, Serbia) for providing the material is also gratefully acknowledged.

References

1. Surappa, M.K.: Aluminium matrix composites: challenges and opportunities. Sadhana 28, 319–334 (2003). doi:10.1007/BF02717141

2. Prasad, S.V., Asthana, R.: Aluminum metal-matrix composites for automotive applications: tribological considerations. Tribol. Lett. 17, 445–453 (2004). doi:10.1023/B:TRIL.0000044492.91991.f3
3. Hunt Jr., W.H., Miracle, D.B.: Automotive applications of metal-matrix composites. In: Miracle, D.B., Donaldson, S.L. (eds.) ASM Handbook, vol. 21: Composites, pp. 1029–1032. ASM International, Materials Park (2001)
4. Vencl, A., Rac, A., Bobić, I.: Tribological behaviour of Al-based MMCs and their application in automotive industry. Tribol. Ind. 26, 31–38 (2004)
5. Goñi, J., Egizabal, P., Coleto, J., Mitxelena, I., Guridi, J.R.: High performance automotive and railway components made from novel competitive aluminium composites. Mater. Sci. Technol. 19, 931–934 (2003). doi:10.1179/026708303225004413
6. Bialo, D., Zhou, J., Duszczyk, J.: The tribological characteristics of the Al-20Si-3Cu-1 Mg alloy reinforced with Al_2O_3 particles in relation to the hardness of a mating steel. J. Mater. Sci. 35, 5497–5501 (2000). doi:10.1023/A:1004833315382
7. Garća-Cordovilla, C., Narciso, J., Louis, E.: Abrasive wear resistance of aluminium alloy/ceramic particulate composites. Wear 192, 170–177 (1996). doi:10.1016/0043-1648(95)06801-5
8. Yang, L.J.: Wear coefficient equation for aluminium-based matrix composites against steel disc. Wear 255, 579–592 (2003). doi:10.1016/S0043-1648(03)00191-1
9. Zou, X.G., Miyahara, H., Yamamoto, K., Ogi, K.: Sliding wear behaviour of Al–Si–Cu composites reinforced with SiC particles. Mater. Sci. Technol. 19, 1519–1526 (2003). doi:10.1179/026708303225007997
10. Korkut, M.H.: Effect of particulate reinforcement on wear behaviour of aluminium matrix composites. Mater. Sci. Technol. 20, 73–81 (2004). doi:10.1179/026708304225011289
11. Miyajima, T., Iwai, Y.: Effects of reinforcements on sliding wear behavior of aluminum matrix composites. Wear 255, 606–616 (2003). doi:10.1016/S0043-1648(03)00066-8
12. Wilson, S., Alpas, A.T.: Effect of temperature on the sliding wear performance of Al alloys and Al matrix composites. Wear 196, 270–278 (1996). doi:10.1016/0043-1648(96)06923-2
13. Sahin, Y., Murphy, S.: The effect of sliding speed and micro-structure on the dry wear properties of metal-matrix composites. Wear 214, 98–106 (1998). doi:10.1016/S0043-1648(97)00201-9
14. Gomes, J.R., Miranda, A.S., Rocha, L.A., Crnkovic, S.J., Silva, V., Silva, R.F.: Tribological behaviour of SiC particulate reinforced aluminium alloy composites in unlubricated sliding against cost iron. In: Proceedings of 2nd World Tribology Congress, Vienna, Austria, CD Presentations/Papers (2001)
15. Vencl, A., Rac, A.: New wear resistant Al based materials and their application in automotive industry. MVM–Int. J. Veh. Mech. Engines Transp. Syst. 30, 115–139 (2004)
16. Sannino, A.P., Rack, H.J.: Dry sliding wear of discontinuously reinforced aluminum composites: review and discussion. Wear 189, 1–19 (1995). doi:10.1016/0043-1648(95)06657-8
17. Soma Raju, K., Bhanu Prasad, V.V., Rudrakshi, G.B., Ojha, S.N.: PM processing of Al–Al_2O_3 composites and their characterisation. Powder Metall. 46, 219–223 (2003). doi:10.1179/003258903225008553
18. Jun, D., Yao-hui, L., Si-rong, Y., Wen-fang, L.: Dry sliding friction and wear properties of Al_2O_3 and carbon short fibres reinforced Al-12Si alloy hybrid composites. Wear 257, 930–940 (2004). doi:10.1016/j.wear.2004.05.009
19. Conley, J.G., Huang, J., Asada, J., Akiba, K.: Modeling the effects of cooling rate, hydrogen content, grain refiner and modifier on microporosity formation in Al A356 alloys. Mater. Sci. Eng. A 285, 49–55 (2000). doi:10.1016/S0921-5093(00)00665-1
20. Mondolfo, L.F.: Aluminium Alloys, Structure and Properties. Butterworths, London (1979)
21. Paes, M., Zoqui, E.J.: Semi-solid behavior of new Al–Si–Mg alloys for thixoforming. Mater. Sci. Eng. A 406, 63–73 (2005). doi:10.1016/j.msea.2005.07.018
22. Yang, X., Jing, Y., Liu, J.: The rheological behavior for thixo-casting of semi-solid aluminum alloy (A356). J. Mater. Process. Technol. 130–131, 569–573 (2002). doi:10.1016/S0924-0136(02)00815-4
23. de Freitas, E.R., Ferracíni Jr., E.G., Piffer, V.P., Ferrante, M.: Microstructure, material flow and tensile properties of A356 alloy thixoformed parts. Mater. Res. 7, 595–603 (2004). doi:10.1590/S1516-14392004000400013
24. ISO 6621–3:2000 Internal Combustion Engines—Piston rings—Part 3: Material specifications (2000)
25. Li, R.X., Li, R.D., Zhao, Y.H., He, L.Z., Li, C.X., Guan, H.R., Hu, Z.Q.: Age-hardening behavior of cast Al–Si base alloy. Mater. Lett. 58, 2096–2101 (2004). doi:10.1016/j.matlet.2003.12.027
26. Straffelini, G., Bonollo, F., Molinari, A., Tiziani, A.: Influence of matrix hardness on the dry sliding behaviour of 20 vol.% Al_2O_3–particulate–reinforced 6061 Al metal matrix composite. Wear 211, 192–197 (1997). doi:10.1016/S0043-1648(97)00119-1
27. Bowen, R., Scott, D., Seifert, W., Westcott, V.C.: Ferrography. Tribol. Int. 9, 109–115 (1976). doi:10.1016/0301-679X(76)90033-5
28. Raadnui, S.: Wear particle analysis—utilization of quantitative computer image analysis: a review. Tribol. Int. 38, 871–878 (2005). doi:10.1016/j.triboint.2005.03.013
29. Ferrography, Texaco Technology Ghent, Ghent (2001)